Chinese Chemical Letters 32 (2021) 2865–2868

Contents lists available at ScienceDirect

Chinese Chemical Letters

journal homepage: www.elsevier.com/locate/cclet

Communication

An intriguing electrochemical impedance aptasensor based on a porous organic framework supported silver nanoparticles for ultrasensitively detecting theophylline

Zhang-Ye Han[a], Hong-Kai Li[a], Qian-Qian Zhu[a], Rongrong Yuan[b], Hongming He[a,*]

[a] Tianjin Key Laboratory of Structure and Performance for Functional Molecules, College of Chemistry, Tianjin Normal University, Tianjin 300387, China
[b] Department of Materials Science and Engineering, Jilin Jianzhu University, Changchun 130118, China

ARTICLE INFO

Article history:
Received 25 November 2020
Received in revised form 4 January 2021
Accepted 6 February 2021
Available online 9 February 2021

Keywords:
Ag@POF composite
Aptamer
Electrochemical aptasensor
Theophylline
Sensitive detection

ABSTRACT

Porous organic frameworks (POFs) are excellently stable porous materials, which can be employed as host platforms to support metal nanoparticles as functional composites for various applications. Herein, a novel POF is successfully prepared *via* Friedel-Crafts reaction. Silver nanoparticles (Ag NPs) are embedded in the prepared POF to generate an Ag@POF composite, which not only possesses high surface area, outstanding physicochemical stability and outstretched π-conjugation skeleton, but also exhibits preferable electrochemical stability and conductivity. This composite is able to immobilize a mass of aptamer strands to fabricate an intriguing electrochemical aptasensor. Electrochemical impedance spectroscopy (EIS) is a commonly used technology to analyze the electrochemical signal variation. The Ag@POF-based biosensor shows the excellent electrochemical detection behavior through analyzing EIS. For instance theophylline as a research mode, the Ag@POF based electrochemical aptasensor reveals ultra-sensitiveness, high selectivity, remarkable stability, good repeatability and simple operability even in various real samples. Notably, this aptasensor has the sensitive detection performance with the limit of detection of 0.191 pg/mL (1.06 pmol/L) in a wide concentration range of 5.0×10^{-4} – 5.0 ng/mL (2.78×10^{-3} – 27.8 nmol/L).

Theophylline (TP) is a commonly used drug for multiple diseases, such as emphysema, cardiac edema, cholecystalgia, bronchial and cardiogenic asthma [1]. The serum concentration of TP significantly affects the pharmacological effect, but the poor drug absorption has an apparent influence of the blood TP concentration due to multi-factors in different individuals, including physical constitution, immune system and disease extent [2]. Low level of TP in blood are poor curative effect, but excessive concentration can cause harmful side-effects on human body [3]. It is worth noting that more than one blood sample (> 25 mL) are usually required for monitoring TP in current clinical practice to result in the difficulty for patients [4]. Therefore, it is vitally important to efficiently and accurately detect TP in a small amount of blood at an ultra-low concentration. Currently, various techniques have been developed to detect TP in clinical laboratory, such as fluorescence polarization immunoassay [5], high performance liquid chromatography [6] and thin layer chromatography [7]. Nevertheless, some obvious disadvantages restrict the broad use of these techniques, for instance operation complex, sample pretreatment, long test time, large volume and expensive equipment. Compare to these test methods, electrochemical sensors have been attracting a range of interest on account of tiny volume, inexpensive facility, excellent detection ability and selectivity [8–11]. Especially, electrochemical aptasensors are greatly potential biosensor for detecting trace analyte due to high sensitivity and selectivity of aptamers [12–14]. In terms of enhancing the detection performance, a variety of functional materials have been prepared and used to cover the working electrode surface to increase the load capacity of aptamer for aggrandizing response signal, such as graphene [15], metal-organic framework [16], metal particle [17] and carbon-based material [18]. Nowadays, exploration and synthesis of more effective functional materials is still a meaningful and challenge research field.

Recently, porous organic frameworks (POFs) have been designed and prepared by covalently-bonded organic motifs with various unique properties, including high surface area, tunable aperturestructure, excellent stability and diversiform structure

* Corresponding author.
E-mail addresses: hehongminghz@163.com, hxxyhhm@tjnu.edu.cn (H. He).

https://doi.org/10.1016/j.cclet.2021.02.013

[19–21]. By virtue of their task-specific features, POFs show greatly potential application values in numerous fields, such as heterogeneous catalysis, gas sorption, sensor [22–24]. Nevertheless, only few POFs are implemented to construct electrochemical sensors for monitoring analytes [25,26], because they always have the poor electroconductibility to restrict their utilizations in electrochemical research. As we know, metal particles have satisfactory electrical conductivity and electrochemical stability, which can be employed as guest species into open structures of POFs to generate composites with the merits of both POFs and metal particles [27,28]. Hence, exploration and development of novel POFs embedded with metal particles has the potential application as biosensors for detecting target analyte.

Encouraged by the above considerations, a novel hyper-crosslinked POF is successfully prepared by the Friedel-Crafts reaction of 1,3,5-tris(bromomethyl)-2,4,6-trimethylbenzene (TBT) and biphenyl (BP). By virtue of the porous structure, the prepared POF can be further employed as a host porous material to confine Ag nanoparticles (Ag NPs) to obtain a Ag@POF composite. Electrochemical impedance spectroscopy (EIS) is always implemented as a useful and sensitive electrochemical response signal to analyze the sensing performance. This composite has outstanding stability, preferable electroconductibility, extend conjugate skeleton and high surface area, leading to immobilizing lots of aptamers to fabricate a highly efficient electrochemical aptasensor in the detection of TP. This composite-based biosensor has super sensitive detection capability, high specificity, superior stability and good repeatability.

There are no any diffraction peaks in the powder X-ray diffraction (PXRD) pattern of POF due to its amorphous solid essence (Fig. 1a). New diffraction peaks at 38.2° and 44.4° in this composite are assigned to (111) and (200) phases of face-centered cubic (fcc) Ag (JCPDS No. 4-0783) [29]. The Ag content in this composite is ~8.3% by using inductively coupled plasma. Thermogravimetric analysis (TGA) show both materials have high thermal stability in air (Figs. S1 and S2 in Supporting information). As seen in Fig. 1b, ^{13}C solid-state NMR spectra exhibit that this composite has the same skeleton structure with the original POF after embedding Ag NPs. Evident signals from aromatic carbons are found from 107 ppm to 145 ppm. The crosslinking process of organic monomers is ascertained by two peaks at 16 and 35 ppm from carbon atoms of bonded methylene and terminal methylene, respectively [30]. Compared to organic monomers, the Fourier transform infrared (FT-IR) spectrum of POF has new infrared absorption characteristic peaks at 2927, 2867 and 1635 $cm^{-1}$from aromatic C–H and CH_2 asymmetric stretching frequencies and the aromatic C=C bond, respectively (Fig. 1c). The FT-IR curve of Ag@POF is similar with that of POF, indicating POF can keep its structure during the synthetic process of Ag@POF. The high-resolution X-ray photoelectron spectroscopy (XPS) of Ag 3d is only found in this composite, which shows two characteristic peaks at 374.6 eV of Ag $3d_{3/2}$ and 368.6 eV of Ag $3d_{5/2}$ (Fig. 1d and Fig. S3 in Supporting information) [31,32]. At the same time, the full XPS spectra of both samples prove that the specific binding energy of Ag only exists in the Ag@POF composite (Figs. S4 and S5 in Supporting information).

N_2 adsorption/desorption isotherms were measured to investigate the internal pore structures. As-synthesized samples were immersed in fresh CH_2Cl_2 for 3 days and further activated at 120 °C for 12 h under vacuum to remove guest molecules. N_2 sorption isotherms of both activated samples show obvious hysteresis loops in the high pressure range on account of internal micro-mesoporous structure (Fig. 2a). The maximum N_2 adsorption amounts of POF and Ag@POF are 406 and 253 cm^3/g at $P/P_0 = 1$ with Brunauer–Emmett–Teller (BET) surface areas of 566 and 462 m^2/g, respectively. The pore size distributions can be analyzed by adopting the non-local density functional theory (Fig. S6 in Supporting information). The apparent decrease of pore volume and N_2 adsorption uptake of this Ag@POF composite is caused by Ag NPs embedded in the porous POF. Scanning electron microscope (SEM) were employed to investigate morphology and microstructure of POF and Ag@POF, illustrating that they are approximate sphere and further accumulated together (Figs. S7 and S8 in Supporting information). Transmission electron microscopy (TEM) images show that Ag NPs are uniformly distributed in the host POF with the particle size from 10 nm to 15 nm (Figs. 2b and c). Furthermore, no any XPS characteristic peaks of P 2p can be found in the as-synthesized Ag@POF, because this sample only has C, H and Ag atoms (Fig. 2d). However, obvious XPS signals of P 2p can be detected in apt/Ag@POF and TP/apt/Ag@POF, confirming the existence of aptamer on the surface of Ag@POF (Figs. 2e and f). The high-angle annular dark field-scanning transmission electron microscopy (HAADF-STEM) with elemental mapping indicate that C and Ag elements from this composite and P element from aptamer are uniform dispersion to prove the successful construction of this electrochemical aptasensor (Figs. 2g–j).

The preparation process of electrochemical aptasensors can be analyzed and explored by using cyclic voltammetry (CV) and EIS electrochemical techniques. The CV curve of bure Au electrode (AE) shows an obvious peak-to-peak separated redox peaks of $[Fe(CN)_6]^{3-/4-}$. However, CV signals exhibit continuous variations of Ag@POF/AE, apt/Ag@POF/AE and TP/apt/Ag@POF/AE (Fig. 3a), because the continuously adding layers of Ag@POF, aptamer and TP can decrease the diffusion coefficient and block the electron transfer between the working electrode surface and the electrolyte solution [33]. The EIS technology is used to discover the impedance change of electrode interface properties [34]. EIS plots can be well simulated by Randles equivalent circuit (Fig. S9 in Supporting information). The R_{ct} value of bare AE is only 0.054 kohm to manifest the clean electrode. Similar with CV results, R_{ct} values gradually enhance to 0.101, 0.179 and 0.346 kohm of Ag@POF/AE, apt/Ag@POF/AE and TP/apt/Ag@POF/AE at 5.0×10^{-4} ng/mL, respectively (Fig. 3b). This electrochemical behavior is principally ascribed to additional cover layers with poor electroconductivity on electrodes [35]. To study the advantage of the Ag@POF-based electrochemical aptasensor, pure POF was also used to modify the working electrode to load aptamers for monitoring TP. The similar signal changes were detected for AE, POF/AE, apt/POF/AE and TP/

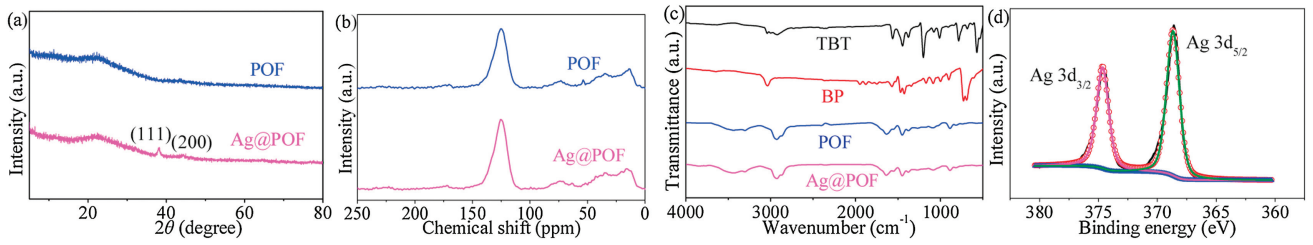

Fig. 1. (a) PXRD patterns, (b) ^{13}C solid-state NMR spectra, (c) FT-IR spectra and (d) the high-resolution XPS spectrum of Ag 3d.

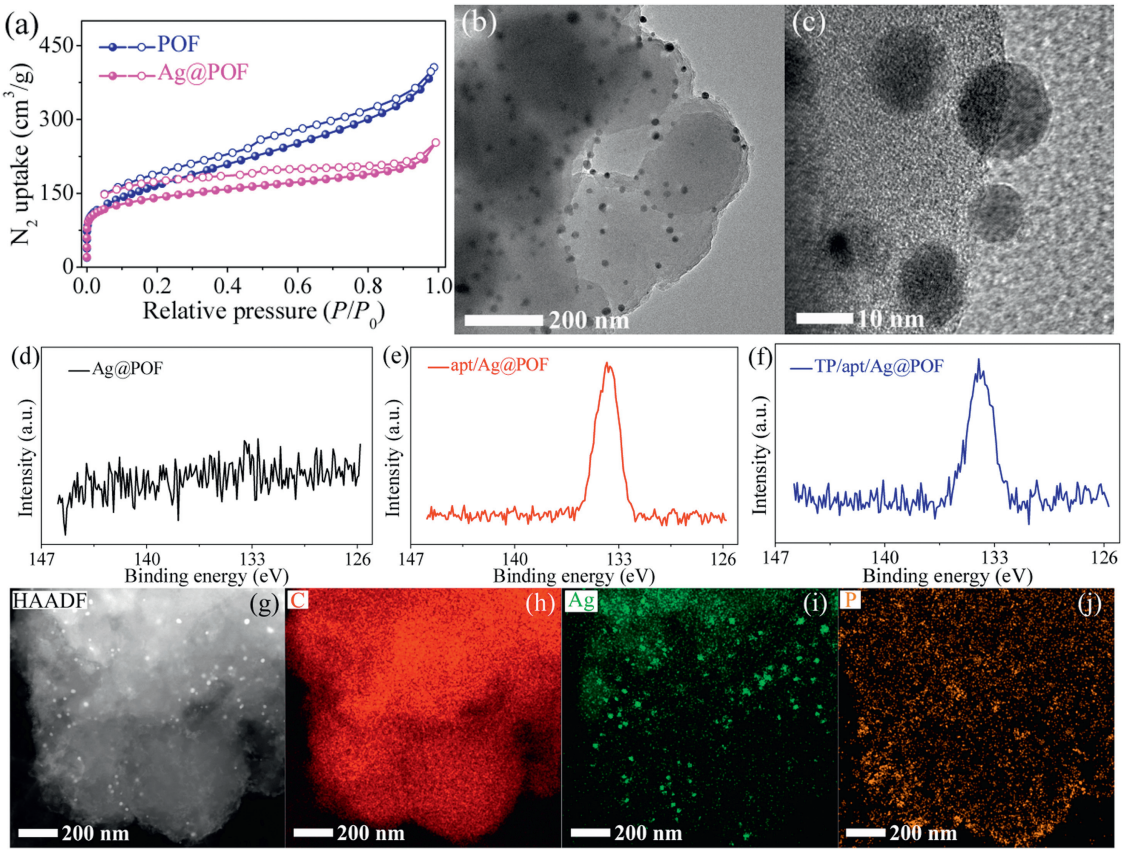

Fig. 2. (a) N_2 sorption isotherms at 77 K. (b, c) TEM images of the Ag@POF composite. High-resolution XPS spectra of P 2p of Ag@POF (d), apt/Ag@POF (e) and TP/apt/Ag@POF (f). (g-j) The HAADF-STEM image of TP/apt/Ag@POF with C, Ag and P elemental mappings.

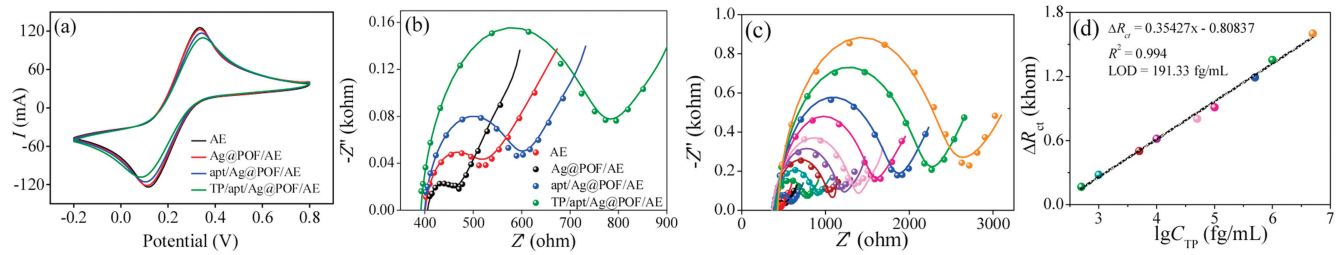

Fig. 3. (a) CV curves and (b) EIS Nyquist plots of different modified AEs. (c) EIS plots of atp/Ag@POF/AE in different TP solutions. (d) The linear dependence of ΔR_{ct} and logarithm values of TP concentration with the fitting straight-line.

apt/POF/AE (Figs. S10 and S11 in Supporting information). The R_{ct} variation (ΔR_{ct}) values of Ag@POF and POF-based electrochemical aptasensors evidently illustrate that the biosensor based on Ag@POF has better electrical conductivity and can load more aptamers for synergistically enhanced electrochemical sensing ability. The corresponding ΔR_{ct} values of POF and Ag@POF as modified materials are 0.111 and 0.047 kohm ($\Delta R_{ct,\ material/AE} - \Delta R_{ct,\ AE}$), and 0.070 and 0.079 kohm ($\Delta R_{ct,\ apt/material/AE} - \Delta R_{ct,\ material/AE}$), and 0.096 and 0.166 kohm ($\Delta R_{ct,\ TP/apt/material/AE} - \Delta R_{ct,\ apt/material/AE}$), respectively (Fig. S12 in Supporting

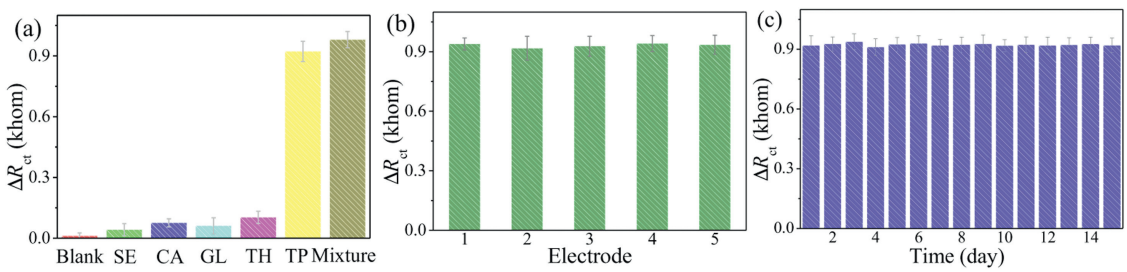

Fig. 4. (a) The selectivity, (b) reproducibility and (c) long-term stability of the prepared Ag@POF-based electrochemical aptasensor towards TP.

information). For exploring the sensing ability of the Ag@POF-based biosensor toward TP, this biosensor was incubated in the TP solution at different concentrations for 30 min and collect the corresponding EIS. The R_{ct} value slowly expands with the gradually increasing TP concentration, because more TP/aptamer compositions can generate on the electrode surface at higher TP concentration to impede the electron transfer between electrolyte and electrode (Fig. 3c). The ΔR_{ct} value of this electrochemical aptasensor before and after soaking in the TP solution is used as response signal to detect TP. There is a good proportional relation between ΔR_{ct} value and logarithm value of TP concentration in the range 5.0×10^{-4} – 5.0 ng/mL (2.78×10^{-3} – 27.8 nmol/L). The linear regression equation can be fitted as $\Delta R_{ct} = 0.35427 \lg C_{TP} - 0.80837$ with a good correlation coefficient (R^2) of 0.994 (Fig. 3d), which is used to calculate the LOD value of 0.191 pg/mL (1.06 pmol/L) with the signal noise ratio of 3. Comparation with other reported materials and methods [36–47], the Ag@POF-based electrochemical aptasensor exhibits excellent sensitive detectability toward TP (Table S1 in Supporting information).

The selectivity of this electrochemical aptasensor based on Ag@POF was investigated by comparing the ΔR_{ct} value of this biosensor in TP or other potential interferences, including serine (SE), caffeine (CA), glucose (GL) and theobromine (TH). The prepared aptasensor has a slight variation after immersing in the interference solutions at 0.1 ng/mL, but an apparent electrochemical impedance variation can be found after exposing in the TP solution at the same concentration (Fig. 4a). This performance can strongly certify that this biosensor possesses the excellent specificity toward TP. The reproducibility was further confirmed by fabricating five electrodes to detect TP (0.1 ng/mL), which have the similar ΔR_{ct} values with the relative standard deviation (RSD) under 5.29% (Fig. 4b). As illustrated in Fig. 4c, this prepared aptasensor can be continuously used to monitor TP at a fix concentration of 0.1 ng/mL for 15 days with the similar detectable ΔR_{ct} value and the RSD value under 6.17% to prove the preferable long-term storage and stability. Consequently, the Ag@POF-based electrochemical aptasensor has outstanding selectivity, preferable reproducibility and acceptable stability in the detection of TP.

The real applicability of the Ag@POF-based electrochemical aptasensor was investigated and analyzed by adding different amounts of TP in real human serum and urine samples. EIS data of this aptasensor toward TP were collected in such real samples by using the standard addition approach. EIS measurements were measured under the same test condition in the pure aqueous solution. The ΔR_{ct} values of apt/Ag@POF/AE toward different TP concentrations in such real samples are similar with the ΔR_{ct} values in the pure aqueous solution (Table S2 in Supporting information). In addition, RSD values are all less than 5.09% and the recoveries are in the range of 98.2%–109.8%. The result illustrates that this Ag@POF-based electrochemical sensor has the preferable detection ability toward TP in human serum and urine.

In this work, an Ag@POF composite is successfully prepared and used as a modified material to fabricate an intriguing electrochemical aptasensor. This biosensor exhibits a super sensitive detection capability toward TP in a wide concentration range by using EIS, which also has excellent selectivity, outstanding stability and good repeatability. More importantly, the electrochemical aptasensor can quantitatively detect TP even in real samples. We hope that this work can provide a representation of POFs embedded metal particles as electrode modification materials to fabricate ultrasensitive electrochemical aptasensors in the quantitative detection of trace target analyte for health and food safety.

Declaration of competing interest

The authors report no declarations of interest.

Acknowledgment

This research was financially supported by the National Natural Science Foundation of China (No. 21801187).

Appendix A. Supplementary data

Supplementary material related to this article can be found, in the online version, at doi:https://doi.org/10.1016/j.cclet.2021.02.013.

References

[1] V. Mastiholimath, P. Dandagi, S.S. Jain, A.P. Gadad, A.R. Kulkarni, Int. J. Pharm. 328 (2007) 49–56.
[2] T.T. Hansel, R.C. Tennant, A.J. Tan, et al., Drug Today 40 (2004) 55–69.
[3] E. Aggelopoulou, S. Tzortzis, F. Tsiourantani, I. Agrios, K. Lazaridis, Med. Princ. Pract. 27 (2018) 387–391.
[4] S. Feng, C. Chen, W. Wang, L. Que, Biosens. Bioelectron. 105 (2018) 36–41.
[5] M. Jolley, J. Anal. Toxicol. 5 (1981) 236–240.
[6] E.A. Abdelaleem, I.A. Naguib, S.A. Farag, H.E. Zaazaa, J. Chromatogr. Sci. 56 (2018) 846–852.
[7] A. Mirfazaelian, M. Goudarzi, M. Tabatabaiefar, M. Mahmoudian, J. Pharm. Pharm. Sci. 5 (2002) 131–134.
[8] F. Gao, J. Song, B. Zhang, et al., Chin. Chem. Lett. 31 (2020) 181–184.
[9] H. Xie, K. Di, R. Huang, et al., Chin. Chem. Lett. 31 (2020) 1737–1745.
[10] Y. Liu, T. Li, C. Ling, et al., Chin. Chem. Lett. 30 (2019) 2211–2215.
[11] W. Zhang, R. Wang, F. Luo, P. Wang, Z. Lin, Chin. Chem. Lett. 31 (2020) 589–600.
[12] G. Xu, J. Hou, Y. Zhao, et al., Sensor. Actuat. B: Chem. 287 (2019) 428–436.
[13] Y. Zhang, G. Figueroa-Miranda, Z. Lyu, et al., Sensor. Actuat. B: Chem. 288 (2019) 535–542.
[14] H. Shi, T. Jin, J. Zhang, et al., Chin. Chem. Lett. 31 (2020) 155–158.
[15] S. Wadhwa, A.T. John, S. Nagabooshanam, A. Mathur, J. Narang, Appl. Surf. Sci. 521 (2020) 146427.
[16] H. He, S.Q. Wang, Z.Y. Han, et al., Appl. Surf. Sci. 531 (2020) 147342.
[17] Y. Song, M. Xu, Z. Li, et al., Sensor. Actuat. B: Chem. 321 (2020) 128527.
[18] Z. Zhang, C. Guo, S. Zhang, et al., Biosens. Bioelectron. 89 (2017) 735–742.
[19] S. Zhang, Q. Yang, C. Wang, et al., Adv. Sci. 5 (2018) 1801116.
[20] H. Ren, G. Zhu, Acta Chim. Sinica 73 (2015) 587–599.
[21] R. Yuan, Z. Yan, A. Shaga, H. He, J. Solid State Chem. 287 (2020) 121327.
[22] T. Ma, X. Zhao, Y. Matsuo, et al., J. Mater. Chem. C 7 (2019) 2327–2332.
[23] J. Yu, S. Chang, X. Xu, X. He, C. Zhang, J. Mater. Chem. C 8 (2020) 8887–8895.
[24] S. Wang, Y. Liu, Y. Ye, et al., Polym. Chem. 10 (2019) 2608–2615.
[25] M.A. Rahman, P. Kumar, D.S. Park, Y.B. Shim, Sensors-Basel 8 (2008) 118–141.
[26] R. Yuan, Z. Yan, A. Shaga, H. He, Sensor. Actuat. B: Chem. 327 (2021) 128949.
[27] A.T.E. Vilian, P. Puthiaraj, C.H. Kwak, et al., Electrochim. Acta 216 (2016) 181–187.
[28] Z.Y. Han, Q.Q. Zhu, H.W. Zhang, R. Yuan, H. He, J. Mater. Chem. C 8 (2020) 14075–14082.
[29] S.P. Deshmukh, A.G. Dhodamani, S.M. Patil, et al., ACS Omega 5 (2020) 219–227.
[30] S. Wang, C. Zhang, Y. Shu, et al., Sci. Adv. 3 (2017) e1602610.
[31] J. Shi, L. Zhang, N. Sun, et al., ACS Appl. Mater. Interfaces 11 (2019) 28858–28867.
[32] A.M. Ferraria, A.P. Carapeto, A.M.B. do Rego, Vacuum 86 (2012) 1988–1991.
[33] Q.Q. Zhu, H.W. Zhang, R. Yuan, H. He, J. Mater. Chem. C 8 (2020) 15823–15829.
[34] Y. Song, F. Duan, S. Zhang, et al., J. Mater. Chem. A 5 (2017) 19378–19389.
[35] X. Yang, C. Zhao, C. Zhang, K. Wen, Y. Zhu, Sensor. Actuat. B: Chem. 323 (2020) 128666.
[36] X. Zhuang, D. Chen, S. Wang, H. Liu, L. Chen, Sensor. Actuat. B: Chem. 251 (2017) 185–191.
[37] X. Chen, Z. Guo, Y. Tang, Y. Shen, P. Miao, Anal. Chim. Acta 999 (2018) 54–59.
[38] W. da Silva, M.E. Ghica, C.M.A. Brett, Anal. Methods 10 (2018) 5634–5642.
[39] X. Gong, C. Yu, Y. Zhang, et al., RSC Adv. 9 (2019) 33898–33902.
[40] B. Mutharani, P. Ranganathan, S.M. Chen, C. Karuppiah, Microchim. Acta 186 (2019) 651.
[41] H.B. Wang, H.D. Zhang, Y.H. Zhang, et al., J. Electrochem. Soc. 162 (2015) B173–B179.
[42] X. Hu, J. Xi, Y. Xia, F. Zhao, B. Zeng, Microchim. Acta 186 (2019) 694.
[43] S.A. Rezvani, A. Soleymanpour, Microchem. J. 149 (2019) 104005.
[44] S. Kesavan, S.A. John, Sensor. Actuat. B: Chem. 205 (2014) 352–362.
[45] G. Yang, F. Zhao, B. Zeng, Talanta 127 (2014) 116–122.
[46] Y.J. Yang, L. Guo, W. Zhang, J. Electroanal. Chem. 768 (2016) 102–109.
[47] S. Kesavan, N.S.K. Gowthaman, S. Alwarappan, S.A. John, Sensor. Actuat. B-Chem. 278 (2019) 46–54.